

# Design of Two-Degree-Of-Freedom (2DOF) Steering Control for Automated Guided Vehicle

Lakpah A. Emmanuel, Christian C. Mbaocha, M. Olubiwe

Department of Electrical and Electronic Engineering, Federal University of Technology, Owerri, Imo State, Nigeria  
Email address: emalala2000@yahoo.com

**Abstract**— Automated Guided Vehicles (AGV) exhibit serious instability in its steering mechanisms, in most cases this results in “snaking” or wavering movement of the vehicle as the speed rises above 5m/s. In order to solve this problem, the steering controller needs to be able to address the two main objective of control, the first one is the set-point tracking and the other one is load disturbance rejection. However, these two aspects conflict with each other practically and cannot be accomplished by the conventional one degree of freedom (1DOF) PID controller. This problem was solved through the use of a two degree of freedom (2DOF) PID controller. The 3-wheels AGV used in this project is modeled using the two-wheel bicycle model to develop the transfer function. The project design work is carried out on Windows 7 platform with MATLAB R2009a software application. This platform was chosen as the version of the application contains the necessary toolboxes to quickly and stably run the necessary simulations. The control strategies was developed and simulated in the SIMULINK environment using the Control Toolbox, and the controller action was viewed, fine-tuned and verified using the PID tuner utility because it provides the capability to carry out auto-tuning of the controller as desired without the rigors involved in manual controller tuning. The simulated result showed great improvement in the final AGV steering controller action in the Rise Time and Settling Time less than 1 second, and overshoot less than 2% of the final value. The control strategies promoted in this work are reference tracking and disturbance rejection. This research will help to stimulate advancement into further development of suitable steering controllers of Automated Guided Vehicles and promote usage in our local industry.

**Keywords**— Automated Guided Vehicles: PID controller: Two Degree of Freedom controller: Load Disturbance Rejection: Two-Wheel Bicycle Model.

## I. INTRODUCTION

The Recent developments in Factory Automation, Computer Integrated Manufacturing Systems, extensive application of Flexible Manufacturing Systems and the introduction of Automatic Warehouses, has seen an elevation in the application of Automated Guided Vehicle (AGV), with remarkable increase in the level of technology, intellectualization, autonomy-oriented, and industrialization. Its extensive usage in discrete logistics systems has made it the necessary tools for the automation of transport systems, monorails, loading and unloading operations, etc. AGV is a branch of mobile robot.

Path tracking and steering control is undoubtedly one of the key technologies in the researching fields of the AGV, because it is very prominent among others, to the successful design and application of an AGV. The steering control system is able to optimize the functioning of the AGV by enabling the following characteristics: smaller tracking error, quick dynamic response, adaptability to complicated circumstances, robustness, etc.

The first AGVs were successfully developed and introduced to the market in 1955 by Barrett Electronics of Northbrook, Illinois, USA. At the time, it was simply a tow truck that followed a wire in the floor instead of a rail. But later, a company named Automation [1] started working on the development of an automatic driverless control system for use in several industrial and commercial applications. Out of this technology came a new type of AGV, which follows invisible UV markers on the floor instead of being towed by a chain. The first such system was deployed at the Willis Tower (formerly Sears Tower) in Chicago, Illinois to deliver mail to its offices [2].

The AGVs have widely been used in industries since their introduction. The number of areas of application and variation in types has increased significantly. Meanwhile, the AGV technology developed rapidly in Europe, Japan, and Korea, because the sizes and structures of pallets for AGV had been standardized. Presently, the AGVs are not only being restricted to internal usage in area such as manufacturing, distribution, and transshipment, but also in outside environments, including the transportation areas [3].

The proportional-integral-derivative (PID) controller is the most common industrial control algorithm. In every process industry, there are two main objective of control, the first one is the set-point tracking and the other one is load disturbance rejection. However, these two aspects conflict with each other practically and cannot be accomplished by the conventional one degree of freedom (1DOF) PID controller. This problem can be solved through the use of a two degree of freedom (2DOF) PID controller. The degree of freedom of a control system is defined as the number of closed-loop transfer functions that can be adjusted independently [1] A two degree of freedom controller has two separate controller units for set-point tracking and disturbance rejection. However, the use of two degree of freedom controllers introduces additional parameters that need to be tuned appropriately.

Two degrees of freedom (2DOF) PID control algorithm has the advantage of elimination of an abrupt change in the control force, and also eliminates the steady state response owing to the input slope and acceleration. Furthermore to employing this control method, the response of the system to unit step disturbance has such low amplitude that approaches to zero [4] These advantages have motivated the use of the 2DOF PID controller for the AGV steering control.

The application of AGV to the Nigerian industry today remains something to be looked upon as a step towards our

desired industrial revolution. The steering controller, being the brain behind the AGV, if locally developed with available resources would set the pace towards achieving this objective.

The smooth operation of an Automated Guided Vehicle (AGV) requires the use of a very effective steering controller. AGV system designs have accommodated several compromises like reducing speeds to very safe levels, centralizing movement authority, and confining the vehicles to dedicated pathways (guide-paths), which are kept clear of obstacles as much as possible, in order to get the AGVs to perform as required. However, such trade-offs to reduce risk oftentimes come at the cost of limitations in performance. Contemporary AGVs rely heavily on specially installed infrastructure to determine their position in the facility where they are used. Such infrastructures are usually costly to install and modify [5]. This has limited the performance of most AGV steering controllers, causing instability and rigorous/complex control action as the vehicle navigates through the desired path. The ability of a steering controller to effectively perform reference tracking, without compromising its ability to reject disturbances, achievable through the use of a two-degree-of-freedom (2DOF) PID controller, would help to overcome the issue of instability at minimal cost.

In this research, the two-degree-of-freedom (2DOF) PID controller, is applied to improving the stability of an Automated Guided Vehicle. The controller is tuned to effectively perform reference tracking and to reject disturbances based on the AGV two-wheel bicycle model.

## II. LITERATURE REVIEW

There has been many previous related research works carried out in the field of automated guided vehicle steering control. In this review, some of the most relevant publications on the said area of research are briefly examined as follows: The components of AGVs that contains three levels of control architecture: vehicle control system, floor control unit and vehicle on-board processor was studied by [6]. A research by [7] investigated how to model automated guided vehicle systems in material handling. AGV Steering wheel system control was improved in a study performed by [8]. A study on Simple Robust Tuning of 2DOF PID Controllers from a Performance/Robustness was carried out by [9]. The authors in [5] developed an Automated Guided Vehicle system that autonomously transported material from loading to unloading stations using robot technology. A parking position detection and control system was developed for precise transshipment of palletized materials between an automated guided vehicle (AGV) and a load transfer station by [10].

Many research gaps are established in the above review of the works in literature. The use of robot technology, localization, and laser coordinate positioning technology to accomplish AGV control would come at a huge design cost, and the absence of most of the materials in the Nigerian market would prove a great limitation in the operability of this control strategy in our immediate environment.

Designing the controller through the use of grid based mapping, and line of sight/cross track error algorithm is limited to very small workspaces, and when considering application of use in large industrial complexes and

warehouses similar to those found in the Nigerian industrial environment, these technology are obviously a far cry from meeting our objectives.

## III. OBJECTIVES OF THE RESEARCH

The main objective of the thesis is: Design of two-degree-of-freedom (2DOF) steering control for Automated Guided Vehicle (AGV). The specific objectives of this research include:

- To determine, with suitable references, the mathematical model of a 3 wheel Autonomous Guided Vehicle using the Ackerman 2-wheel bicycle model
- Design a 2DOF compensator/controller for the vehicle model using SIMULINK library in MATLAB
- Tune the overall system steering controller for disturbance rejection and reference tracking to achieve the design specification using the PID tuner utility in SIMULINK

## IV. MATHEMATICAL MODEL OF AGV

The methods used to achieve improved linearized mathematical models of the AGV steering controller based on two-wheel bicycle are presented in this section. The state space representation and transfer function of two-wheel bicycle mathematical models are achieved. The materials/tools used during this research are: MATLAB, SIMULINK interface and other related research tools.

At higher vehicle speeds, the assumption that the velocity at each wheel is in the direction of the wheel can no longer be made. In the case of this research, instead of a kinematic model, a dynamic model for lateral vehicle motion is used.

The lateral direction of the vehicle is the sideways moving direction of the vehicle, which can be measured with respect to the vehicle and with respect to a fixed reference point. The longitudinal direction is the forward moving direction of the vehicle. Fig. 1.0 is the vehicle lateral dynamics showing the lateral and longitudinal axes.

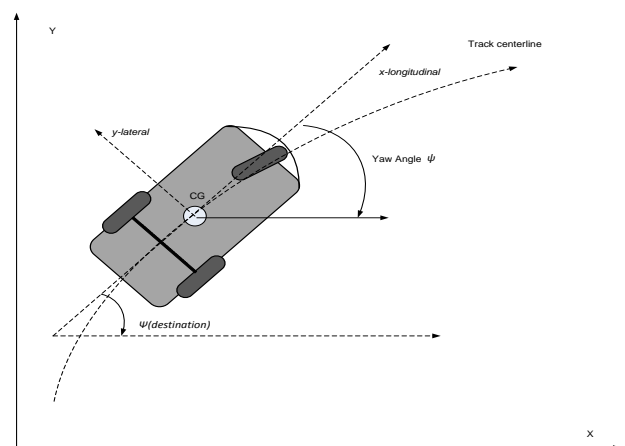


Fig. 1.0. Lateral Vehicle Dynamics

The continuous time state model for the two input vehicle model is a system given as the 2DOF bicycle model [11]. Three coordinates are required to describe the motion of the vehicle: X, Y, and  $\psi$ . X, Y are inertial coordinates of the location of the C.G of the vehicle while  $\psi$  describes the

orientation of the vehicle. This requires some basic assumptions.

**A. AGV Two-Wheel Bicycle Model Assumptions**

In order to model the AGV using the two-wheel bicycle model, several assumptions must be held true. These assumptions considered are:

- 2-DoF, Lateral position,  $y$  (measured from instantaneous center of rotation O), Yaw,  $\psi$  (with respect to Global Axis)
- Longitudinal velocity  $V_x$  is assumed to be constant.
- Small slip angles, i.e. tires operate in the linear region.
- No rear wheel steering.
- No aligning moment in both tires.
- No road gradient or bank angle.
- There are only two wheels, one in the front and one in the rear (the two rear wheels consolidated as one).
- No lateral and longitudinal load transfer
- No rolling and pitching motion
- No chassis or suspension compliance effects

**B. Vehicle Coordinate System**

The global vehicle coordinate system is shown in Fig. 2.0. The position vector for body and wheel are:

$y_b=(r_b,\theta_b)$  and  $y_w=(r_w,\theta_w)$  respectively. The relative wheel position vector with respect to the chassis frame is:

$$y_{w/b}=(r_{w/b},\theta_{w/b}) \tag{1}$$

The subscript ‘b’ refers to the chassis local vector, the subscript ‘w’ refers to the wheel local vector and the subscript ‘w/b’ refers to the relative vector between wheel and chassis.

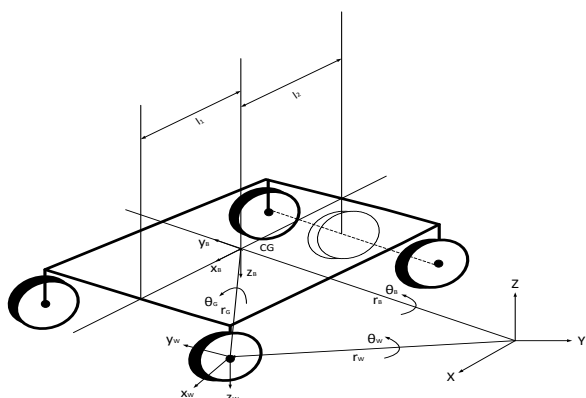


Fig. 2.0. Vehicle model coordinate system

**C. Bicycle Model Notations**

Table 1.0 shows the notations that would be used to model the vehicle.

For simplicity, as shown in Fig. 3.0, the lateral forces of each wheel pair of the rear axle are added into one force  $F_{xr}$ , and for the front steering wheel  $F_{xf}$ . The same applies for the longitudinal forces  $F_{yf}$  and  $F_{yr}$ .

Lateral Acceleration of CG in the G frame ( relative vector between wheel and chassis)	$a_y$
Lateral Acceleration of CG in the B frame (chassis/body local vector)	$\ddot{y}$
Yaw angle	$\psi$
Yaw rate	$\dot{\psi}$
Longitudinal Velocity of Vehicle	$V_x$
Front/Rear Tire Cornering Stiffness	$C_{\alpha_f} C_{\alpha_r}$
Front/Rear Tire Slip Angle	$\alpha_f \alpha_r$
Front/Rear wheel Steering Angle	$\delta_f \delta_r$
Front/Rear Wheel Velocity Angle	$\theta_{vf} \theta_{vr}$
Distance from CG to Rear/Front Axels	$L_f, L_r$
Vehicle Length	$L=L_f+L_r$
Road Radius	$R$
Front Lateral Tire Force	$F_{yf}$
Rear Lateral Tire Force	$F_{yr}$
Moment of Inertia	$I_z$
Lateral Velocity of Vehicle	$V_y$
Mass	$m$
Lateral Forces in the W frame (wheel local vector)	$F_{cr}, F_{cf}$
slip angle	$\beta$

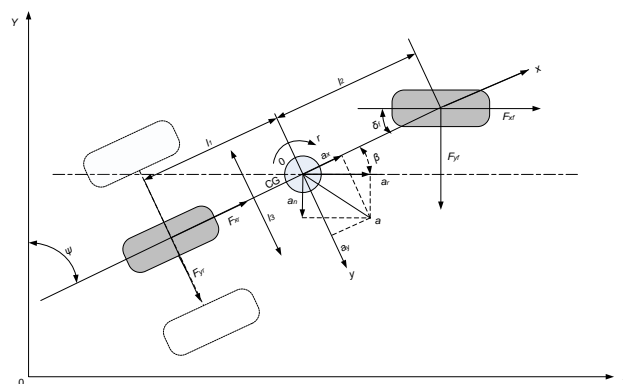


Fig. 3.0. Ackerman Reduced Bicycle model

Fig. 4.0 shows the equivalent 2-wheel bicycle model used to model the 3-wheel Automated Guided vehicle.

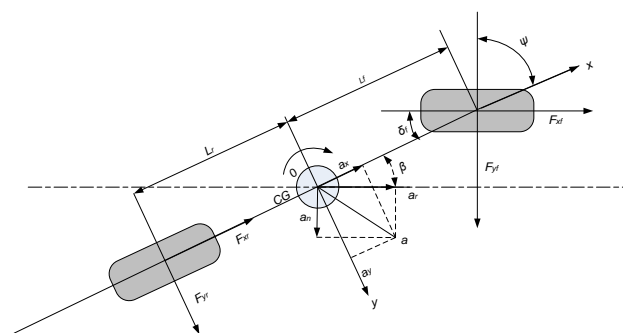


Fig. 4.0. Side Track Model for Vehicle Lateral Dynamics

The two degrees of freedom are represented by the vehicle lateral position  $y$  and the vehicle yaw angle  $\psi$ . The vehicle

lateral position is measured along the lateral axis of the vehicle to the point 0 which is the center of rotation of the vehicle. The vehicle yaw angle  $\psi$  is measured with respect to the global x-axis. The longitudinal velocity of the vehicle at the center of gravity (C.G) is denoted by  $V_x$ .

#### D. System Single-Track Bicycle Modeling

The single-track bicycle model, also known as the Ackerman simplified model, is used for modeling the vehicle. Using the diagram in Fig. 4.0, considering the lateral force equilibrium, ignoring road bank angle and applying Newton's second law of motion along the y axis, gives the equation for the lateral translational motion of the vehicle as in (2.0).

$$Ma_y = F_{yf} + F_{yr} \quad (2.0)$$

$$= \left( \frac{d^2 y}{dt^2} \right) \quad (3.0)$$

Where  $a_y$  is the inertial acceleration of the vehicle at the center of gravity (C.G.) in the direction of the y-axis and,  $F_{yf}$  and  $F_{yr}$  are the lateral tire forces of the front and rear wheels respectively.

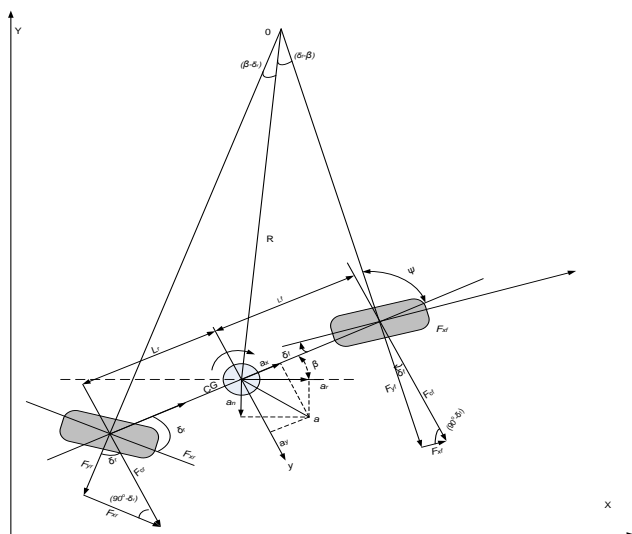


Fig. 5.0. Kinematics of lateral vehicle motion

From Fig 5.0, considering lateral forces (chassis/body local vector), it follows that:

$$F_{yr} = F_{cr} \cos \delta_r \text{ \& } F_{yf} = F_{cf} \cos \delta_f \quad (4.0)$$

The lateral force denoted by  $F_{cf}$  is called the cornering force when the camber angle is equal to zero. At a given tire load, the cornering force increases with a slip angle. Hence, the equation for the lateral translational motion of the vehicle is defined as:

$$ma_y = F_{cf} \cos \delta_f + F_{cr} \cos \delta_r = C_{af} \alpha_f \cos \delta_f + C_{ar} \alpha_r \cos \delta_r \quad (5.0)$$

Where, the parameters are as defined in table 1.0. The slip angle of the tire is the angle between the orientation of the tire and the orientation of the velocity vector of the wheel. In Fig 6.0 the Slip Angle of the front tire is  $\alpha_f$ .

The next step is to model the lateral tire forces that act on the vehicle for the front tire  $F_{yf}$  and the rear tire  $F_{yr}$ . The

velocity angle  $\theta_{vf}$  is the angle the velocity vector makes with the longitudinal axis of the vehicle. The front wheel steering angle is  $\delta_f$ .

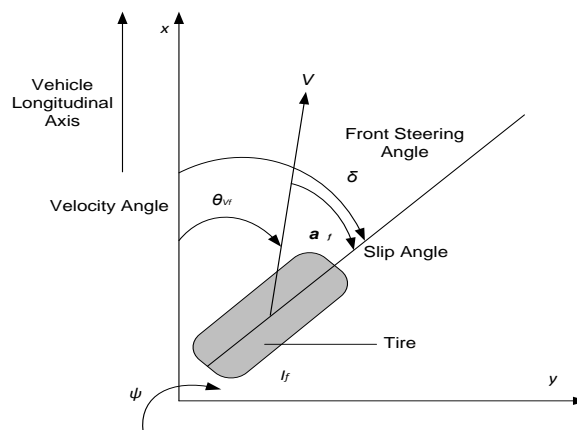


Fig. 6.0. Front Tire Slip Angle

The lateral tire force is proportional to the slip angle (when the slip angle is small). Considering the front tires, referring to Fig 5.0 and Fig 6.0, the front lateral tire force is shown in (6.0).

$$F_{yf} = C_{af} \left( \delta_f - \frac{\gamma + L_f \psi}{V_x} \right) \quad (6.0)$$

Considering the rear tires, the rear lateral tire force is defined as in (7.0).

$$F_{yr} = C_{ar} \left( \delta_r - \frac{\gamma - L_r \psi}{V_x} \right) \quad (7.0)$$

Having derived the parameters for the front and rear tires, ignoring the road bank angle and applying Newton's second law of motion along the y-axis, the exact lateral force balance is defined as in (8.0).

$$m(\ddot{y} + V_x \dot{\psi}) = C_{af} \left( \delta_f - \tan^{-1} \left( \frac{\dot{y} + L_f \dot{\psi}}{V_x} \right) \right) \cos \delta_f + C_{ar} \left( \delta_r - \tan^{-1} \left( \frac{\dot{y} - L_r \dot{\psi}}{V_x} \right) \right) \quad (8.0)$$

Assuming that  $\theta_{vr}$  and  $\theta_{vf}$  are small, to obtain the approximate lateral force balance as in (9.0).

$$\ddot{y} = \left( -\frac{2C_{ar} + C_{af}}{mV_x} \right) \dot{y} + \left( \frac{2C_{ar}L_r + C_{af}L_f}{mV_x} - V_x \right) \dot{\psi} + \frac{C_{af}}{m} \delta_f \quad (9.0)$$

Considering the rear wheels, the approximate moment balance equation is presented as in (10.0).

$$\ddot{\psi} = \frac{L_f C_{af} \delta_f}{I_z} + \frac{2C_{ar}L_r - C_{af}L_f}{I_z V_x} \dot{y} - \frac{2C_{ar}L_r^2 - C_{af}L_f^2}{I_z V_x} \dot{\psi} \quad (10.0)$$

#### E. State Space Representation

In order to describe the dynamic behavior of the bicycle model, a state space model will be used, which can easily be derived from the equations of motion. The state space model can be written in (11.0) and (12.0).

$$\dot{x} = Ax + Bu \quad (11.0)$$

$$y = Cx + Du \quad (12.0)$$

The state space representation for the system is given as in (13.0) and (14.0).

$$\begin{Bmatrix} \ddot{\gamma} \\ \ddot{\psi} \end{Bmatrix} = \begin{bmatrix} -\frac{2C_{ar} + C_{af}}{mV_x} & \frac{2L_r C_{ar} + L_f C_{af}}{mV_x} - V_x \\ \frac{2L_r C_{ar} + L_f C_{af}}{I_z V_x} & \frac{2L_r^2 C_{ar} + L_f^2 C_{af}}{I_z V_x} \end{bmatrix} \begin{Bmatrix} \dot{\gamma} \\ \dot{\psi} \end{Bmatrix} + \begin{bmatrix} \frac{C_{af}}{m} \\ \frac{C_{af} L_f}{I_z} \end{bmatrix} \delta_f \quad (13.0)$$

The system initial output is:

$$\begin{Bmatrix} a_y \\ \ddot{\psi} \end{Bmatrix} = \begin{bmatrix} -\frac{2C_{ar} + C_{af}}{mV_x} & -\frac{2L_r C_{ar} + L_f C_{af}}{mV_x} \\ 0 & 1 \end{bmatrix} \begin{Bmatrix} \dot{\gamma} \\ \dot{\psi} \end{Bmatrix} + \begin{bmatrix} \frac{C_{af}}{m} \\ 0 \end{bmatrix} \delta_f \quad (14.0)$$

#### F. Vehicle Parameters

The vehicle parameters to be used in this project design is that of CLAAS Renault ARES 640 provided in a research by [12]. The parameters are given in table 2.0.

TABLE 2.0: Vehicle parameters

Parameters	Values
$v_x$	10m/s (Dorf R, 2011)
$C_{af}$	34378N/rad
$C_{ar}$	71620N/rad
$L_f$	1.88m
$L_r$	1.0m
$m$	8000kg
$I_z$	11051kgm

#### G. Vehicle Transfer Function

The transfer function equation is defined between the steering angle input and a yaw rate output. The vehicle transfer function is obtained by substituting the values of the vehicle parameters in table 2.0 into the state space presentation of the vehicle model obtained in (13.0) and (14.0). The resulting equations are shown in (15.0) and (16.0).

$$\begin{Bmatrix} \ddot{\gamma} \\ \ddot{\psi} \end{Bmatrix} = \begin{bmatrix} -2.22 & -9.02 \\ 0.711 & 2.4 \end{bmatrix} \begin{Bmatrix} \dot{\gamma} \\ \dot{\psi} \end{Bmatrix} + \begin{bmatrix} 4.29 \\ 5.85 \end{bmatrix} \delta_f \quad (15.0)$$

The system output equation is:

$$\begin{Bmatrix} a_y \\ \ddot{\psi} \end{Bmatrix} = \begin{bmatrix} -2.22 & -0.98 \\ 0 & 1 \end{bmatrix} \begin{Bmatrix} \dot{\gamma} \\ \dot{\psi} \end{Bmatrix} + \begin{bmatrix} 4.29 \\ 0 \end{bmatrix} \delta_f \quad (16.0)$$

The overall system transfer function matrix in concatenated form is then given as (17.0).

$$G(s) = \begin{bmatrix} G_1(s) \\ G_2(s) \end{bmatrix} \quad (17.0)$$

Where the transfer function from input to output using the MATLAB syntax (sys=tf(G)) is given in (18.0) and (19.0).

$$G_1(s) = \frac{4.29s^2 - 3.28s + 160.4}{s^2 - 0.12s - 1.751} \quad (18.0)$$

$$G_2(s) = \frac{5.85s + 16.04}{s^2 - 0.12s - 1.751} \quad (19.0)$$

Therefore, putting (18.0) and (19.0) in (17.0) the transfer function matrix is now as in (20.0).

$$G(s) = \begin{bmatrix} \frac{4.29s^2 - 3.28s + 160.4}{s^2 - 0.12s - 1.751} \\ \frac{5.85s + 16.04}{s^2 - 0.12s - 1.751} \end{bmatrix} \quad (20.0)$$

The transfer function obtained is that of a MIMO system, where one input 'front steering angle' yields two possible outputs: 'lateral acceleration 1 and 2' on different frames. For

the purpose of path tracking and disturbance rejection, the transfer function  $G_1$  (lateral acceleration 1) would be used for the remainder of this research as follows:

For  $V_x = 5m/s$ ,

$$\begin{Bmatrix} \ddot{\gamma} \\ \ddot{\psi} \end{Bmatrix} = \begin{bmatrix} -4.44 & -3.03 \\ 1.42 & 4.79 \end{bmatrix} \begin{Bmatrix} \dot{\gamma} \\ \dot{\psi} \end{Bmatrix} + \begin{bmatrix} 4.29 \\ 5.85 \end{bmatrix} \delta_f \quad (21.0)$$

and,

$$\begin{Bmatrix} a_y \\ \ddot{\psi} \end{Bmatrix} = \begin{bmatrix} -4.44 & -1.79 \\ 0 & 1 \end{bmatrix} \begin{Bmatrix} \dot{\gamma} \\ \dot{\psi} \end{Bmatrix} + \begin{bmatrix} 4.29 \\ 0 \end{bmatrix} \delta_f \quad (22.0)$$

For  $V_x = 15m/s$ ,

$$\begin{Bmatrix} \ddot{\gamma} \\ \ddot{\psi} \end{Bmatrix} = \begin{bmatrix} -1.48 & -14.34 \\ 0.48 & 1.6 \end{bmatrix} \begin{Bmatrix} \dot{\gamma} \\ \dot{\psi} \end{Bmatrix} + \begin{bmatrix} 4.29 \\ 5.85 \end{bmatrix} \delta_f \quad (23.0)$$

and,

$$\begin{Bmatrix} a_y \\ \ddot{\psi} \end{Bmatrix} = \begin{bmatrix} -4.48 & -0.66 \\ 0 & 1 \end{bmatrix} \begin{Bmatrix} \dot{\gamma} \\ \dot{\psi} \end{Bmatrix} + \begin{bmatrix} 4.29 \\ 0 \end{bmatrix} \delta_f \quad (24.0)$$

These transfer functions from (21.0) to (24.0) represents the plant (vehicle), at different fixed longitudinal velocity that would be used later for comparison and result analysis.

### V. AGV CONTROLLER DESIGN

In this section the 2DOF compensator/controller for the AGV is design to improve the system model.

#### A. Design Requirements

In this research, the movement of the AGV through the desired path was tracked and rejected the unstable movement along the guided path by manipulating the steering, in consonance with the error generated by the rear wheels offset from the desired path. The overall design requirements are to:

Track a sudden increase of 1.0 step in the reference signal setpoint (Reference Tracking). The detailed design requirements are:

- Settling time under 5 seconds
- Steady-state error to the step reference input less than 10%
- Overshoot below 0.5%

Reject a 0.5 unit sudden increase in the disturbance from a SIMULINK step block (Disturbance Rejection). The detailed design requirements are:

- Settling time under 2 seconds
- Peak deviation from steady state below 0.5

The design would be a 2DOF PID controller (2DOF) in the PID Tuner platform implemented in SIMULINK, and used to achieve the desired responses in both reference tracking and disturbance rejection.

#### B. AGV System MATLAB Design

The overall AGV system model design in SIMULINK environment is shown in Fig 7.0. The Subsystems are created by using a Subsystem Block in SIMULINK. The Subsystem blocks are added to the and also the transfer function blocks  $G_1$  and  $G_2$  to make up the subsystem. The signal builder block in SIMULINK allows for creation of interchangeable groups of piecewise linear sources and use them in a model.

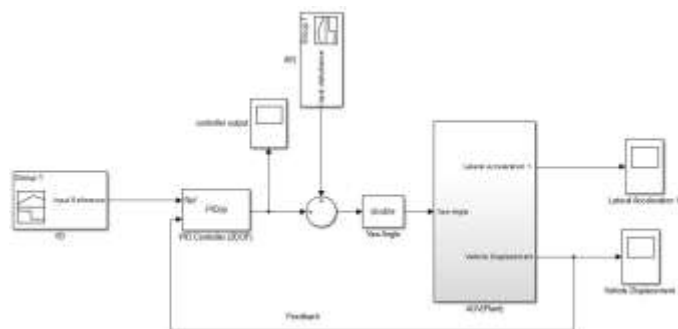


Fig. 7.0. Overall System Model Design in SIMULINK

The model used here would utilize the signal builder block to create the input reference signal (setpoint) and the input disturbance signal. The input reference signal to be used is as unit step input. The signal would run for 10 seconds, starting at 0 and increases to 1 after 1 sec. the controller would be designed to track this input signal changes and tuned to meet the design specification. The input disturbance signal to be used is a unit step input. The signal would run for 10 seconds, increases its amplitude to 0.5 after 5 seconds. The controller would be designed to reject this input disturbance changes and tuned to meet the design specification.

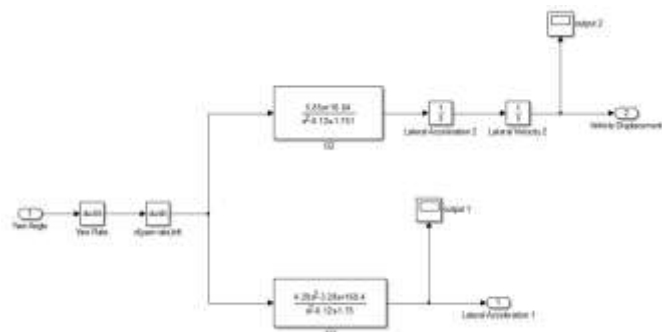


Fig. 8.0. AGV Subsystem SIMULINK Model Design

The PID Tuner provides step plot for different loop responses such as reference tracking (from  $r$  to  $y$ ) and controller efforts (from  $r$  to  $u$ ), etc. From Fig 7.0, the disturbance occurs after the 2DOF pre-filter, this justified that the input disturbance rejection plot that assumes a step disturbance occurs at the input of the AGV plant model. Fig 8.0 is a detailed look under the mask of the AGV model design.

## VI. RESULTS AND DISCUSSION

The results obtained from the simulation and tests conducted on the AGV model using the 2DOF PID controller are discussed in this section.

### A. Initial Condition Results

To obtain the desired results from the design, there is need to determine the initial conditions of the plant (AGV). To achieve this, the AGV model if simulated before the controller is tuned and the initial conditions are shown in Fig. 9.0

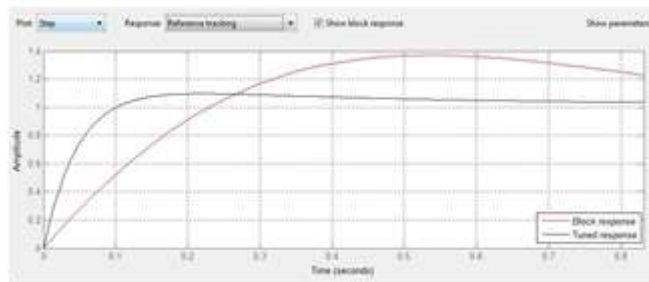


Fig. 9.0. Initial System Reference Tracking Results (graphical)

The readings from fig 9.0 are shown in tables 3.0 and 4.0.

TABLE 3.0: Initial System Tuning Parameters

Parameter	Tuned
P	4.0959
I	0.86186
D	--0.0014905
N	2747.96
b	1
c	1

TABLE 4.0: Initial System Reference Tracking Results

Parameters	Tuned	Block
Rise Time	0.0715 seconds	0.179 seconds
Settling Time	0.978 seconds	1.72 seconds
Overshoot	8.6%	37.1%
Peak	1.1	1.37

The PID tuner automatically designs an initial PI controller. The controller gains and performance metrics are shown in Table 4.0.

For reference tracking, the overshoot is 8.6%, which is not in line with the design objectives at this stage when compared to the design requirements (Section V).

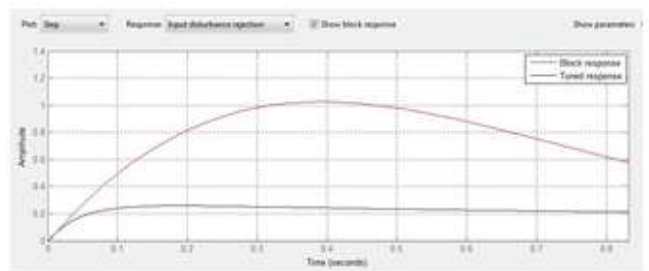


Fig. 10.0. Initial System Input Disturbance Rejection Results

TABLE 5.0: Initial System Input Disturbance Rejection Results

Parameters	Tuned	Block
Rise Time	0 seconds	0 seconds
Settling Time	17.9 seconds	3.53 seconds
Overshoot	Inf (<1)	Inf (<1)
Peak	0.259	1.03

Similarly, for input disturbance rejection results are shown in Table. 5.0. The settling time is 17.9 sec. and the overshoot is below the zero reference line (inf.), which is also not corresponding with the design specification (Section V).

### B. Reference Tracking Result

The initial design is tested on the nonlinear model (controller + plant) by applying it in the PID Tuner. This writes the parameters back to the PID block in the SIMULINK

model and the effects on reference tracking are shown in Fig 11.0.

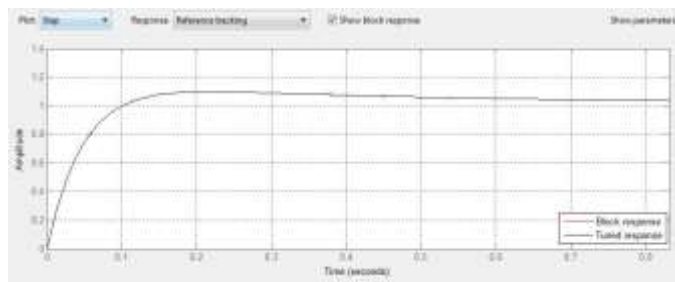


Fig. 11.0. System Reference Tracking Results After Initial Tuning

The parameters clearly shows that the 1.1(10%) peak deviation from steady state and overshoot of 8.6% are still not as expected, hence the need to tune the controller further to improve its performance and robustness.

TABLE 6.0: System Reference Tracking Results After Initial Tuning

Parameter	Tuned
Rise Time	0.0715 seconds
Settling Time	0.978 seconds
Overshoot	8.6%
Peak	1.1

The peak deviation would have to be reduced by at least 10% using the PID Tuner. The closed loop response of the controller is obtained by applying the tuned parameters to the controller and running the model SIMULINK.

### C. Disturbance Rejection Result

The initial design when tested on the nonlinear model (controller + plant) by applying it in the PID Tuner would write the parameters back to the PID block in the SIMULINK model and the effects on disturbance rejection is shown in Fig 12.0 and Table 7.0.

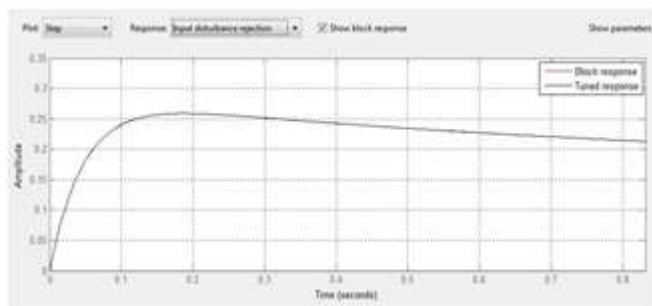


Fig. 12.0. System Disturbance Rejection Results after initial tuning

TABLE 7.0: System Disturbance Rejection Results after initial tuning

Parameters	Results
Rise Time	0 seconds
Settling Time	17.9 seconds
Overshoot	Inf (<1)
Peak	0.259

The parameters in Table 7.0 show that the overshoot (<1) is still not as expected, also the large settling time of 17.9 seconds does not conform with the requirement hence the need to further tune the controller to improve its performance and

robustness. The settling time would have to be reduced below 2 seconds using the PID Tuner.

### D. Controller Result at Different Velocities

The diagrams in Fig. 13.0 to Fig. 16.0 represent the 2DOF steering controller and plant (AGV) response to a unit step input at three different lateral velocities namely: 5m/s and 15m/s.

At  $V_x=5\text{m/s}$ ,  $P=46.28$ ,  $I=98.63$ ,  $D=-0.0420$ ,  $N=243$ , and the system stabilized after 0.00483 sec. See Fig 13.0 and Fig 14.0.

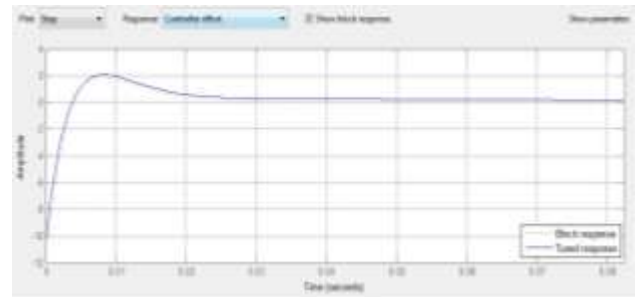


Fig. 13.0. Controller performance at  $V_x=5\text{m/s}$

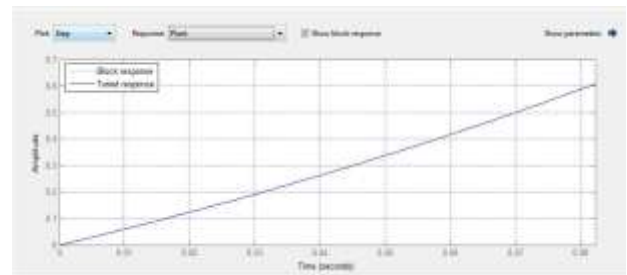


Fig. 14.0. Plant (Vehicle) behavior at  $V_x=5\text{m/s}$

At  $V_x=15\text{m/s}$   $P=41.24$ ,  $I=77.48$ ,  $D=-0.0470$ ,  $N=214.2$  and the system stabilized after 0.0295 seconds. See Fig 15.0 and Fig 16.0.

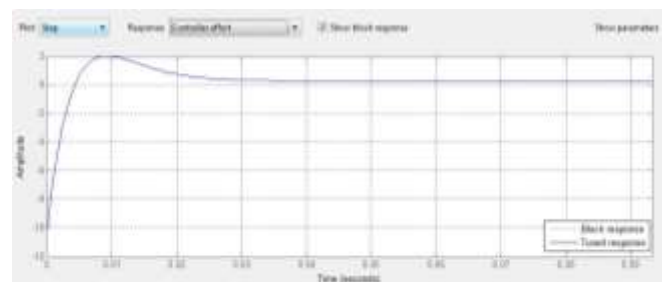


Fig. 15.0. Controller performance at  $V_x=15\text{m/s}$

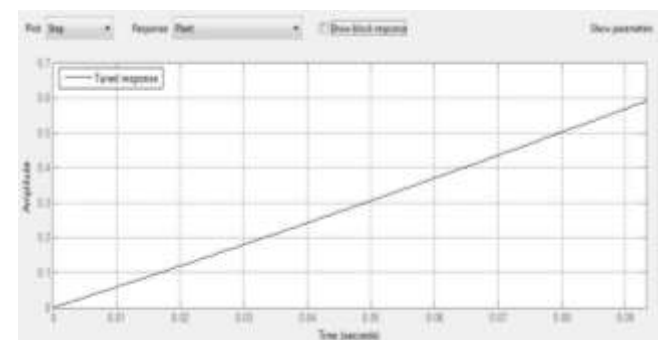


Fig. 16.0. Plant (Vehicle) behavior at  $V_x=15\text{m/s}$

It is observed that at lower velocities the controllers tend to have higher gains and achieves its setpoint faster. This is in contrast with higher velocities where the controller gains,  $N$  are lower and the controller takes relatively more time to attain stability. At  $V_x = 15\text{m/s}$ , the disparity between the actual and desired path becomes more obvious, and as such the system would require even longer time with more iterations to entirely match the setpoint. The rise time and settling time for both input disturbance rejection and reference tracking also increased with increasing longitudinal velocity of the vehicle

#### E. Overall System Performance and Test Result

The diagram in Fig 17.0 shows the response pattern of the AGV as it moves through the path, given a unit step command before tuning

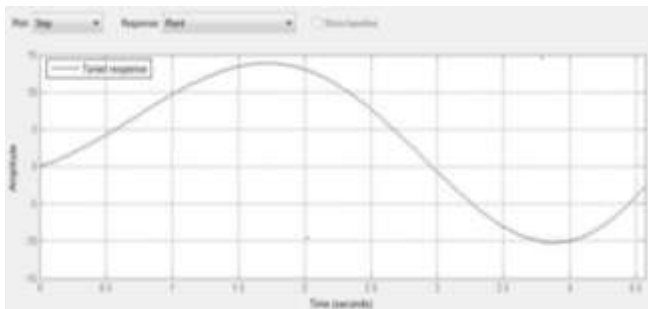


Fig. 17.0 Vehicle (plant) motion pattern before Tuning

In contrast to the “snaking” movement of the vehicle previously, the diagram in Fig 17.0 shows the smooth movement of the AGV through the same path when subjected to the unit step command. It is in form of a normalized rise. The tuned response represents the actual path of the vehicle after controller tuning action.

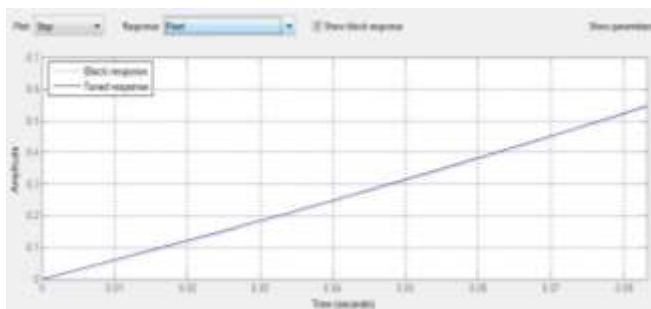


Fig. 18.0 Vehicle Trajectory after tuning with 2DOF PID controller

With the input disturbance rejection and reference tracking performances having met the design requirements, the result is a smooth longitudinal velocity of the AGV with good performance and robustness.

#### VII. CONCLUSION

It is imperative to state that the use of a 2DOF PID controller design to control the steering of an Automated Guided Vehicle successfully achieved a balanced performance in reference tracking and disturbance rejection. A more robust and higher accuracy in the saturation region is obtained with the introduction of the 2DOF PID control filter to the plant (AGV) rather than the traditional linear PID controller. This

has helped to eliminate any form of wavering movement or “snaking” of the AGV as it moves along the desired path. The PID Tuner was used to tune and achieve good disturbance rejection and tracking.

The recommendation for further work on this research is the validation of the steering control strategy with field tests on particular AGV model and obtaining quantifiable results from this physical implementation of the controller for comparison/improvement.

#### REFERENCES

- [1] Horowitz I. M., “Synthesis of Feedback Systems”, Academic Press, 5(2), 113–127, 1963.
- [2] Yuedong Zhan, Youguang Guo, and JianGuo Zhu, “Intelligent Coordination Steering Control of Automated Guided Vehicle Vision-based”, IEEE 3(6) 2011.
- [3] Butdee, S., Suebsomran, A., Vignat, F., and Yarlagadda, P.K.D.V., “Control and path prediction of an Automate Guided Vehicle”, Journal of Achievements in Materials and Manufacturing Engineering, Vol.31 (2), 2008.
- [4] Ogata, K., “Modern Control Engineering, Prentice-Hall”, 3(5), 558–567, 1997.
- [5] Sajjad Yaghoubi, Sanam Khalili, Reza Mohammad Nezhad, Mohammad Reza Kazemi, and Mahsa Sakhaifar., “Designing and Methodology of Automated Guided Vehicle Robots/ Automated Guided Vehicles Systems”, Future Trends, IJRRAS. Vol.13 (1), 2012 .
- [6] Falcone .P, Borrelli .F, Asgari, J., Tseng, H. E., and Hrovat, D., “Predictive Active Steering Control for Autonomous Vehicle Systems”, IEEE Transaction of Control Systems Technology, 11(4) 147-156, 2007.
- [7] Büilent Sezen, “Modeling Automated Guided Vehicle Systems in Material Handling” Dogus Oniversiiesi Dergisi,4 (2) 207-216, 2003.
- [8] Achille, S., Sathish Kumar, R., “Automated Guided Vehicle, ACET, 8(5), 2016.
- [9] Alfaro, V.M. and Vilanova, R., “Simple Robust Tuning Of 2DOF PID Controllers from a Performance/Robustness Trade-Off Analysis”, Asian Journal of Control, 15(5), 1–14, 2013.
- [10] Xing Wu, Pei Huang Lou, Ke Shen, Guangqing Peng, and Dunbing Tang, “Precise Transshipment Control of an Automated Magnetic-Guided Vehicle Using Optics Positioning”, International Journal on Smart Sensing and Intelligent Systems, 5(3) 210-224, 2014.
- [11] Gurkan Erdogan, “Vehicle Planar Dynamics – Bicycle Model”, 5(6), 80–85, 2011.
- [12] Ehsan Kiani, “Design and Development of an Auto-Steering System Control for Off-Road Vehicles”, Eastern Mediterranean University, 2012.